Proc. Natl. Acad. Sci. USA
Vol. 91, pp. 7578–7582, August 1994
Neurobiology

Clustering of Ca^{2+} channels and Ca^{2+}-activated K^+ channels at fluorescently labeled presynaptic active zones of hair cells

(auditory system/confocal microscopy/electrical tuning/fluo-3/vestibular system)

NAOUM P. ISSA AND A. J. HUDSPETH

Howard Hughes Medical Institute and Center for Basic Neuroscience Research, University of Texas Southwestern Medical Center, Dallas, TX 75235-9117

Contributed by A. J. Hudspeth, April 12, 1994

ABSTRACT **Electrical resonance, which in some hair cells provides a mechanism for frequency tuning, is mediated by clusters of Ca^{2+} channels and Ca^{2+}-activated K^+ channels that have been proposed to occur at presynaptic active zones. To localize Ca^{2+} channels on the cellular surface, we loaded hair cells from the frog's sacculus with the Ca^{2+} indicator fluo-3 and imaged them by fluorescence confocal microscopy. When a cell was depolarized, we observed on its basolateral surface several foci of transiently enhanced fluorescence due to local Ca^{2+} influx. After protracted recording, each cell displayed on average 18 brightly and permanently fluorescent spots at the same positions. We mapped these spots in four hair cells and compared their locations with those of presynaptic active zones, as determined from transmission electron micrographs of serial sections through the same cells. The results demonstrated that enhanced fluo-3 fluorescence marks active zones. Measurement of currents through membrane patches at fluorescently labeled active zones demonstrated that both voltage-activated Ca^{2+} channels and Ca^{2+}-activated K^+ channels occur there. These results confirm that the ion channels involved in electrical tuning and synaptic transmission by hair cells cluster together at presynaptic active zones.**

Hair cells, the sensory receptors of the internal ear, in many instances respond preferentially to specific frequencies of mechanical stimulation. Frequency selectivity is mediated by several processes acting independently or in concert (for a review, see ref. 1). One of these mechanisms, electrical tuning (for a review, see ref. 2), relies on the interaction of a voltage-activated Ca^{2+} current and a Ca^{2+}-activated K^+ current (3–6). When mechanical stimulation of the hair bundle elicits an excitatory response (for a review, see ref. 7), the resulting depolarization activates voltage-gated Ca^{2+} channels. The ensuing influx of Ca^{2+} further depolarizes the cell and rapidly increases the Ca^{2+} concentration near the channels. The elevated local Ca^{2+} concentration, in turn, opens Ca^{2+}-activated K^+ channels that congregate with the voltage-gated Ca^{2+} channels (8, 9). The outward flow of K^+ repolarizes the cell, closing Ca^{2+} channels and priming the cell for another cycle of oscillation. The number, distribution, and kinetics of Ca^{2+} channels and K^+ channels determine the characteristic frequency at which a cell best responds (2, 6).

Two lines of evidence suggest that the Ca^{2+} and K^+ channels involved in electrical tuning are colocalized at the hair cell's presynaptic active zones (8). First, the distribution of channel clusters resembles that of active zones: scattered over the basolateral surface of a hair cell from the leopard frog's sacculus, there are ≈20 channel clusters and ≈20 presynaptic active zones. Second, all of the voltage-activated Ca^{2+} channels of these hair cells occur in clusters with Ca^{2+}-activated K^+ channels; any process requiring voltage-gated Ca^{2+} channels, including synaptic transmission, must therefore use the same set of channels.

The presynaptic active zones of hair cells resemble those of other cells, such as photoreceptors and electroreceptors, that conduct quantal neurotransmitter release in response to graded membrane potentials. Such an active zone characteristically displays a prominent osmiophilic dense body adjacent to the presynaptic membrane. At the afferent synapse of hair cells, this dense body is spherical or ellipsoidal, with a diameter of 250–1000 nm (10–14). The dense body is surrounded by clear-cored synaptic vesicles, which may be attached to it by fine strands. The inner aspect of the plasmalemma at an active zone displays a prominent presynaptic density; at the hair cell's synapse, this structure comprises several parallel bars of filamentous material, whose pattern corresponds to the array of intramembrane particles in the presynaptic membrane (8, 12, 14, 15).

Physiological studies of presynaptic active zones have heretofore been impeded by the absence of a means of identifying active zones in living cells. In this study, we report a technique for identification of individual presynaptic active zones in living hair cells (16). Using this method, we have verified that Ca^{2+} channels and K^+ channels congregate at active zones.

MATERIALS AND METHODS

Preparation. Hair cells were generally isolated from the sacculus of the leopard frog (*Rana pipiens*); a few experiments were performed on the bullfrog (*Rana catesbeiana*). The saccular macula was dissected and placed for 15 min at room temperature in 0.5 g of papain (Sigma) per liter in low-Ca^{2+} saline solution (110 mM Na^+/2 mM K^+/100 μM Ca^{2+}/110 mM Cl^-/3 mM D-glucose/5 mM Hepes, pH 7.25). After a further 15 min in the same solution without enzyme, the otolithic membrane was mechanically removed; hair cells were then teased from the macula with an eyelash and allowed to settle on a concanavalin A-coated coverslip. Dissociated cells were maintained at room temperature, ≈21°C, in oxygenated standard saline solution identical to that above save for the presence of 4 mM Ca^{2+} and 118 mM Cl^-.

Electrophysiological Recordings. Whole-cell, tight-seal recordings were conducted with a patch-clamp amplifier (EPC-7, List Electronics, Darmstadt, Germany) connected to an experimental interface (LM-900, Dagan Instruments, Minneapolis) controlled by a personal computer (486ZXP, Northgate Computer Systems, Minneapolis) running electrophysiological software (AXOBASIC, Version 1.0, Axon Instruments, Burlingame, CA). Whole-cell pipettes had resistances of 3–5 MΩ when filled with an internal solution containing 104 mM K^+, 2 mM Na^+, 2 mM Mg^{2+}, 104 mM Cl^-, 1 mM ATP, and 5 mM Hepes (pH 7.3). The internal solution additionally contained the Ca^{2+} indicator fluo-3 (17) at a concentration of 100–200 μM (pentaammonium salt, Molecular Probes). This

The publication costs of this article were defrayed in part by page charge payment. This article must therefore be hereby marked "*advertisement*" in accordance with 18 U.S.C. §1734 solely to indicate this fact.

indicator usually filled the cytoplasm within 1–2 min after the onset of whole-cell recording.

Dual recordings were conducted by the simultaneous use of whole-cell and patch electrodes (8). The current across a cell-attached membrane patch was monitored through a pipette of resistance 2–3 MΩ, filled with standard saline solution. A second voltage-clamp amplifier maintained this pipette's potential at ground. The seal resistances of cell attached patches ranged from 50 MΩ to several gigaohms.

Cells were held at voltages between −70 mV and −50 mV and periodically were depolarized by 56 mV to activate Ca^{2+} currents fully (5). To remove linear leakage and capacitive currents, each current response was subjected to P/4 correction. After being filtered with an eight-pole Bessel filter (852, Wavetek, San Diego) set at a half-power frequency of 2.5 kHz, currents were sampled at 10 kHz.

Confocal Microscopy. After being loaded with fluo-3 through tight-seal whole-cell pipettes, hair cells were imaged by means of a laser-scanning confocal-illumination system (MRC-600, Bio-Rad) attached to an inverted microscope (IM-35, Zeiss) equipped with a ×63 oil-immersion objective lens of numerical aperture 1.4. Images were simultaneously acquired through two channels and stored for later analysis. A fluorescein filter pack (BHS, Bio-Rad) was used in the imaging of fluo-3 fluorescence, while transmitted laser light was sampled through differential-interference-contrast optics appropriately oriented with respect to the laser beam's plane of polarization. The depth of confocal sectioning along the optical axis was estimated at 1 μm for the fluorescence system. To ensure adequate sampling when the positions of presynaptic active zones were to be determined, the focus motor was advanced through 0.6-μm or 1-μm steps between successive images.

Electron Microscopy. After the completion of physiological recording, an isolated hair cell to be examined by electron microscopy was fixed on a coverslip for 30 min at room temperature in 200 mM glutaraldehyde/5 mM $CaCl_2$/80 mM sodium cacodylate, pH 7.4. The specimen was then postfixed for 30 min at 0°C with 31 mM OsO_4/4 mM $CaCl_2$/64 mM sodium cacodylate, pH 7.4. After partial dehydration, a preparation was stained *en bloc* for 60 min with 0.5% uranyl acetate in 95% ethanol. The sample was then dehydrated, transferred through propylene oxide, and embedded in epoxy plastic (EMbed 812, Electron Microscopy Sciences, Fort Washington, PA). The cell was located by reference to fiducial marks transferred to the plastic surface from the scored coverslip. Serial ≈100-nm sections were examined and photographed with an electron microscope (JEM-1000, JEOL) operated at an accelerating voltage of 80 kV.

RESULTS

Fluo-3 Fluorescence on the Hair Cell's Basolateral Surface. In an attempt to localize presynaptic active zones by identifying the sites where Ca^{2+} enters the hair cell's cytoplasm through voltage-sensitive channels, we loaded hair cells with the Ca^{2+} indicator fluo-3 and observed them by confocal fluorescence microscopy. During the first few minutes after establishment of the whole-cell recording condition, the basolateral periphery of a cell held at a membrane potential of −70 mV typically displayed modest fluo-3 fluorescence (Fig. 1*A*). Depolarizing the cell to −14 mV elicited an inward ionic current followed by a considerably larger outward current (Fig. 1*D*); previous experiments have demonstrated these components to traverse respectively Ca^{2+} channels and Ca^{2+}-activated K^+ channels (3–5). During the depolarization, several regions adjacent to the plasmalemma at the cell's basolateral surface became strongly fluorescent (Fig. 1*B*). When the cell was repolarized to −70 mV, these regions dimmed to a level near their initial intensity (Fig. 1*C*).

Three control experiments (data not shown) suggested that Ca^{2+} current was required to elicit the increase in fluorescence during depolarization. When a hair cell was depolarized to +80 mV, a potential sufficiently positive to suppress the influx of Ca^{2+}, no change was observed in the cell's fluorescence. Next, when the extracellular Ca^{2+} concentration was reduced by local application of Ca^{2+}-free saline solution through a coarse pipette, the fluorescence increase during depolarization was again eliminated. Finally, as the Ca^{2+} current "washed out" over time, depolarization ceased to modulate the intensity of the fluorescence. An outward K^+ current was not required for the increase in fluorescence; brightening occurred in response to depolarization in cells loaded with internal solution in which K^+ was replaced by 100 mM Cs^+ (data not shown), which blocks Ca^{2+}-activated K^+ channels.

Pattern of Enduring Fluo-3 Fluorescence. Over the course of 5–15 min after the indicator had diffused into a cell, several regions permanently became much brighter than the remainder of the soma. In addition to the highly fluorescent nucleus,

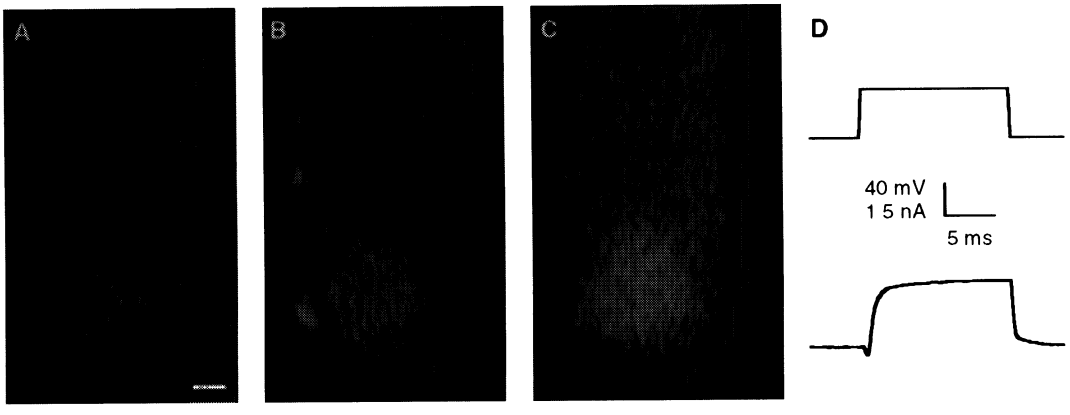

FIG. 1. Depolarization-induced increases in fluorescence intensity on a hair cell's basolateral surface. (*A*) Within the first few minutes of an experiment, a cell loaded with fluo-3 and maintained at a membrane potential of −70 mV displayed weak fluorescence. (Bar = 2 μm in *A*, *B*, and *C*.) (*B*) While a confocal image was acquired over 190 ms by scanning along the vertical axis, the same cell was subjected to a 15-ms depolarization to −14 mV. Several regions along the basolateral cellular surface displayed transient increases in Ca^{2+} concentration, as reflected by enhanced fluo-3 fluorescence. (*C*) Immediately after the conclusion of the train of depolarizing pulses the bright regions disappeared. The same regions subsequently became permanently labeled by fluo-3. (*D*) A train of 10 depolarizing voltage commands (upper trace), including that used while acquiring the image in *B*, evoked biphasic ionic currents (average in lower trace). This and all succeeding figures involve cells from the leopard frog.

10–35 spots of intense fluorescence were observed along the cell's basolateral surface. These bright spots were adjacent to the plasmalemma and appeared to be spherical, with a diameter of 300–500 nm (Fig. 2*A*). Bright spots appeared both in cells subjected to depolarizations and in those continuously maintained at −70 mV. In every instance in which prolonged observations were made, a region that first brightened transiently during membrane depolarization subsequently displayed a permanently fluorescent spot. When a cell was examined by differential-interference-contrast microscopy, a spherical, refractile structure of the same size and position as a bright spot was usually observed (Fig. 2*B*).

We mapped the intensely fluorescent spots in individual hair cells by acquiring 10–20 confocal sections at 1-μm intervals, which together spanned the entire depth of a cell. Superposing all of the optical sections from one hair cell revealed fluorescent spots over the basolateral two-thirds of the cellular surface (Fig. 2*C*). Bright spots often appeared in pairs (Fig. 2*D*). A hair cell of the leopard frog's sacculus contained an average of 18 ± 4 (mean ± SD; n = seven cells) membrane-associated bright spots.

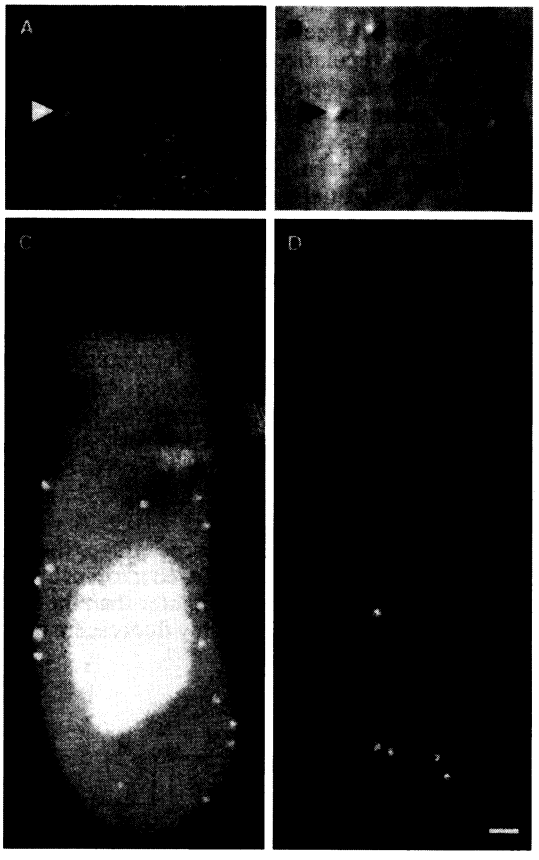

FIG. 2. Light-microscopic detection and distribution of presynaptic structures in a saccular hair cell: (*A*) In a confocal fluorescence image taken after several minutes of recording, a hair cell loaded with 200 μM fluo-3 and held at a membrane potential of −70 mV displayed an intensely fluorescent spot adjacent to the plasma membrane. (*B*) When imaged with differential-interference-contrast optics, the cell showed a spherical structure in the same position as the bright spot. (Bar = 2 μm in *B* and *A*.) (*C*) The images from 18 confocal sections, which sampled the entire thickness of an isolated hair cell, were superposed to show the distribution of intensely fluorescent spots. Although some bright spots appear to lie near the cell's center, they actually occurred upon either the upper or the lower aspect of the cell. This cell had 22 bright spots, 6 of which were concealed by the strong fluorescence of the nucleus. The fluorescent structure at the upper right of the cell is the whole-cell recording pipette. (*D*) A single confocal section, taken at the bottom surface of a cell loaded with fluo-3, displayed two pairs of bright spots. (Bar = 2 μm in *D* and *C*.)

Colocalization of Fluorescent Spots and Presynaptic Active Zones. The distribution of brightly fluorescent spots resembles that of afferent synapses on the hair cell's basolateral surface (8, 15). To determine whether the fluorescent spots in fact occur at presynaptic active zones, we compared three-dimensional fluorescence maps and transmission electron micrographs of the same cells. Four hair cells, three from leopard frogs and one from a bullfrog, were loaded with fluo-3, and their fluorescent spots were completely mapped in three dimensions with the confocal microscope. The cells were then fixed, embedded, serially sectioned, and examined in a transmission electron microscope. Presynaptic active zones were identified by three morphological features: a spherical, ≈400-nm dense body, a surrounding ring of synaptic vesicles, and a presynaptic density at the plasma membrane (Fig. 3*C*). Because of shrinkage during fixation and embedding, the electron-microscopic images of cells did not have dimensions identical to those of confocal images. Bright spots in confocal sections were therefore correlated with presynaptic dense bodies if they appeared in the same order in the through-cell series of sections, and at the same relative position with respect to morphological landmarks such as the cellular boundary, nucleus, and cuticular plate. In this analysis, we excluded bright spots that occurred at positions corresponding to sections lost during preparation for electron microscopy, which often encompassed the 1–2 μm of a cell closest to the coverslip. Because the cell surface apposed to a coverslip was flattened, it generally contained several bright spots (see Fig. 2*B*) that were lost.

The positions of fluorescent spots were highly correlated with those of presynaptic active zones (Fig. 3; Table 1). Of 45 bright spots observed in four cells, 38 coincided with active zones detected by transmission electron microscopy. Of 41 active zones observed by electron microscopy, only 3 lacked obvious bright spots at the corresponding positions in confocal maps. In the case of 8 other bright spots or presynaptic active zones, the correlation was ambiguous because of uncertainty in identifying either a bright spot in confocal images or a presynaptic dense body in electron micrographs.

Colocalization of Fluorescent Spots and Channel Clusters. The increase in fluorescence intensity associated with Ca^{2+} currents suggested that bright spots mark membrane regions

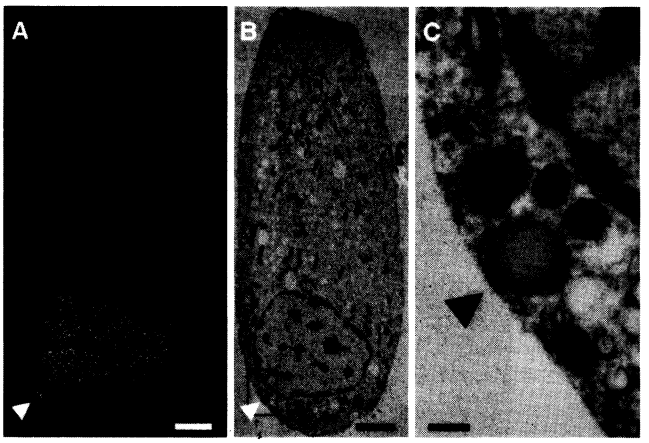

FIG. 3. Fluo-3 fluorescence at presynaptic active zones. (*A*) A confocal section of a living hair cell loaded with fluo-3 demonstrated an intensely fluorescent spot (arrowhead) at the cellular periphery. (*B*) A transmission electron micrograph of the same cell confirmed the presence of a presynaptic active zone at the position of the bright spot in *A*. (*C*) An enlargement of the presynaptic active zone in *B* displays the features characteristic of a hair cell's afferent synapse: a spherical presynaptic dense body 420 nm in diameter, a halo of clear-cored synaptic vesicles, and a presynaptic density. (Bar = 2 μm in *A* and *B* and 200 nm in *C*.)

Table 1. Colocalization of intensely fluorescent spots and presynaptic active zones

Species	Cell surface area, μm^2		Bright spots, no.			Active zones without associated bright spots	Questionable identity	Total no. of bright spots in cell
	Basolateral	Lost in sectioning	Lost in sectioning	Associated with active zones	Not associated with active zones			
R. pipiens	571	145	1	12	1	1	0	14
	544	170	5	5	2	0	2	12–14
	628	184	5	9	1	1	1	15–16
R. catesbeiana	603	112	1	12	3	1	5	16
Total	2346	611	12	38	7	3	8	57–60

The basolateral surface areas of four hair cells were estimated by measuring the lengths of membrane profiles in transmission electron micrographs with no correction for shrinkage during histological preparation. The "questionable identity" column enumerates instances in which the identity of either a bright spot or a presynaptic active zone was in doubt.

with high Ca^{2+}-current densities. Because K^+ channels are known to cluster with Ca^{2+} channels in hair cells (8), channels of both types might be expected to occur near each bright spot. To examine this possibility, we used a dual voltage-clamp system (8) to measure the fraction of the whole-cell current that flowed across the membrane patch immediately adjacent to a bright spot. While one voltage-clamp amplifier recorded the entire cell's current, a second amplifier measured only the current flowing through the patch.

Depolarization through the whole-cell recording pipette induced measurable ionic currents in 12 of 21 membrane patches examined at bright spots. Fig. 4 shows one cell's total ionic current as well as the current through a patch of membrane contiguous to a bright spot. Because the fluorescent spots presented small targets for electrode positioning, the pipettes visibly failed to encompass the bright spots in many recording attempts. In every such case (14 of 14 patches), no ionic current was observed. Moreover, none of 15 membrane patches randomly chosen without the aid of fluo-3 fluorescence exhibited appreciable ionic current.

Patch currents shared several features with whole-cell currents. There were usually two components to each, an early, inward Ca^{2+} current followed by a larger, outward K^+ current. Patch currents activated and deactivated with essentially the same time courses as whole-cell currents (Fig. 4). Furthermore, the Ca^{2+} components of whole-cell and patch currents washed out at the same rate (data not shown). Patch currents ranged in magnitude from 1% to 6% of the simultaneously recorded whole-cell currents. Because a patch current seems to be a miniature version of the whole-cell current, it is probable that the whole-cell current reflects the summed currents from several membrane patches, each with a similar number of clustered Ca^{2+} and K^+ channels.

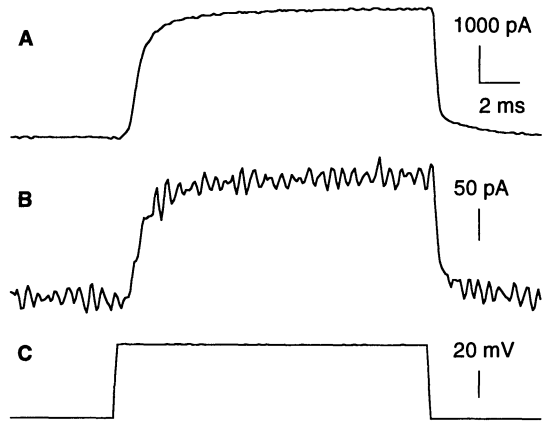

FIG. 4. Currents measured simultaneously by whole-cell and patch electrodes. (*A*) Depolarization evoked a whole-cell current in which the Ca^{2+}-activated K^+ current greatly exceeded the Ca^{2+} current. Electronic compensation was applied for the cellular capacitance and for 60% of the series resistance of ≈15 MΩ. (*B*) Elicited by the same depolarization as in *A*, the current through a membrane patch at a presynaptic active zone was measured with a tight-seal patch electrode situated at a brightly fluorescent spot. This patch current displayed a time course similar to that of the simultaneously recorded whole-cell current. In the steady state, the patch current was ≈6% of the whole-cell current; the hair cell correspondingly had 16 brightly fluorescent spots. (*C*) The responses above were elicited by 10 15-ms depolarizations from −60 mV to −4 mV.

DISCUSSION

Using a combination of confocal microscopy and transmission electron microscopy, we have demonstrated that spots of intense fluo-3 fluorescence in hair cells correspond to presynaptic active zones. The observation of enhanced fluo-3 fluorescence at these sites provides a means of studying active zones that is far less labor-intensive than serial section electron microscopy and can be applied in living cells. By measuring currents across the membrane adjacent to such fluorescent spots, we have demonstrated that both Ca^{2+} and K^+ channels occur there. Taken together, these findings confirm the suggestion (8, 9) that the Ca^{2+} and K^+ channels responsible for electrical tuning in the frog's saccular hair cell are clustered at presynaptic active zones.

Might the coincidence of bright spots and presynaptic active zones have been fortuitous? If the two structures were randomly and independently distributed, the binomial distribution can be used to calculate the probability of our observations' having occurred by chance. Assuming random distributions of bright spots and active zones in 2-μm^2 bins, the probability of finding both structures in the same bin is ≈5%; instead, 38 of 45 bins containing bright spots also held active zones. If the locations of bright spots and active zones were not correlated, the probability of the observed number of coincidences (or more) would therefore be $<10^{-41}$; the fluorescent spots almost certainly correspond to presynaptic active zones.

Labeling of Presynaptic Active Zones in Living Hair Cells. Presynaptic active zones seem to be labeled by fluo-3 by two distinct processes. In healthy cells that displayed little prior fluorescence, activation of whole-cell Ca^{2+} currents transiently increased the intensity of fluo-3 fluorescence at active zones. Clustering of Ca^{2+} channels at the hair cell's presynaptic active zones would be expected to raise the cytoplasmic Ca^{2+} concentration to very high levels in the small region involved in vesicle release (9, 18, 19); we believe that the transient increase in fluorescence reflects this local increase in Ca^{2+} concentration.

After prolonged exposure to fluo-3, presynaptic active zones became permanently and specifically labeled by the indicator. The basis of this permanently enhanced fluorescence is unknown. It is possible that fluo-3 preferentially binds to presynaptic dense bodies. Because neither the molecular composition (but see ref. 20) nor the function of

dense bodies is known, however, it is unclear why the indicator might become concentrated in those structures. Moreover, dense bodies are not membrane-bounded and therefore cannot maintain an elevated local concentration of free Ca^{2+} in the absence of Ca^{2+} influx. Another possible basis for permanent labeling is that fluo-3 enters synaptic vesicles; although we used the charged form of the indicator in our experiments, fluo-3 has been shown to gain access to some membrane-bound organelles (21). The enhanced fluorescence might thus reflect intravesicular accumulation either of the indicator or of Ca^{2+} (22).

Colocalization of Ca^{2+} and K^+ Channels with Presynaptic Active Zones. Because fluo-3 fluorescence reliably marks presynaptic active zones in living cells, we were able to study the ionic currents at identified active zones. When bright spots served as targets for electrode placement, the probability of measuring a significant ionic current in a membrane patch increased from <6% to 57%. When a bright spot or its differential-interference-contrast correlate could clearly be seen within a patch pipette, a significant patch current was almost always observed. When a patch pipette obviously missed a bright spot, however, ionic current was never measured. Although the basolateral membrane of the frog's hair cell bears some solitary channels (5), the results indicate that most of the Ca^{2+} channels and Ca^{2+}-activated K^+ channels are clustered at the hair cell's presynaptic active zones.

Our recordings from cell-attached patches at presynaptic active zones demonstrated currents with many characteristics of those involved in electrical tuning. The patch-current amplitudes were variable, however, and generally smaller than would be predicted from division of the whole-cell current by the number of active zones per cell. Loose-seal patch recordings, in which no membrane bleb was pulled into the pipette, suggested that each active zone contributes a larger fraction, on average ≈8%, of the whole-cell current (8). These discrepancies may be attributed to the contorted state of the presynaptic membrane induced by tight-seal formation and to variability in the holding potential in our patch recordings due to uncompensated access resistance.

Bright spots were stationary during the course of recordings from intact hair cells. Sometimes, however, a cell produced blebs, or focal separations of its plasma membrane and cortex from the cytoskeleton. In many such cases, bright spots and spherical, refractile structures of the same diameter were found associated with the detached membrane. In one instance, a bleb bearing such a spherical structure was pulled into a pipette; the resultant cell-attached patch displayed Ca^{2+} and K^+ currents. These results suggest that the presynaptic dense body and associated ion channels are interconnected through components of the cellular cortex (23, 24).

Significance for Synaptic Signaling. Fluorescence confocal microscopy afforded us a convenient means of mapping the distribution of presynaptic active zones in hair cells. In agreement with earlier electron-microscopic results (13, 15, 25, 26), our data showed that active zones often appear in pairs. This arrangement may serve as a means of strengthening the synaptic connection between a hair cell and a particular afferent terminal. Within a given type of hair cell, active zones are generally of similar dimensions. The synaptic strength in such cells may be enhanced, not by production of larger active zones, but by deployment of more.

K^+ channels terminate presynaptic excitation in many neurons (27–31). In hair cells that do not employ electrical resonance as a tuning mechanism (32, 33), K^+ channels may serve the same function that such channels do in neuronal terminals. In hair cells whose characteristic frequencies are determined by electrical resonance, however, the interaction of Ca^{2+} and K^+ channels additionally provides band-pass filtering and amplification of inputs (4, 6). The role of K^+ channels in electrical tuning by hair cells may therefore be regarded as a specialized adaptation of a widespread, phylogenetically ancient synaptic regulatory mechanism.

The hair cell's afferent synapse affords a useful system for biophysical experimentation on presynaptic functions. Each active zone has a stereotyped pattern of presynaptic structures and a similar complement of Ca^{2+} and Ca^{2+}-activated K^+ channels. Because such an active zone can now readily be identified in a living cell, tight-seal recording may be used to study the behavior of ion channels known to lie in a patch of presynaptic membrane. The rise and fall of presynaptic Ca^{2+} concentration can be investigated with high temporal and spatial resolution by the use of fluorescent dyes. Finally, it should be possible to measure at a single synapse the capacitance changes resulting from exocytotic fusion of synaptic vesicles, perhaps even of individual vesicles.

Dr. A. McDowall and Messrs. D. Bellotto and R. A. Jacobs kindly assisted the authors with electron microscopy. Dr. S. C. Cannon provided software that was modified for our experimentation. For comments on the manuscript, we thank the members of our laboratory group and Drs. D. W. Hilgemann, L. F. A. Jaramillo, F. N. Katz, K. Luby-Phelps, and W. M. Roberts. National Institutes of Health Grant DC00317 supported this research.

1. Roberts, W. M., Howard, J. & Hudspeth, A. J. (1988) *Annu. Rev. Cell Biol.* **4**, 63–92.
2. Fettiplace, R. (1987) *Trends Neurosci.* **10**, 421–425.
3. Lewis, R. S. & Hudspeth, A. J. (1983) *Nature (London)* **304**, 538–541.
4. Art, J. J. & Fettiplace, R. (1987) *J. Physiol. (London)* **385**, 207–242.
5. Hudspeth, A. J. & Lewis, R. S. (1988) *J. Physiol. (London)* **400**, 237–274.
6. Hudspeth, A. J. & Lewis, R. S. (1988) *J. Physiol. (London)* **400**, 275–297.
7. Hudspeth, A. J. (1989) *Nature (London)* **341**, 397–404.
8. Roberts, W. M., Jacobs, R. A. & Hudspeth, A. J. (1990) *J. Neurosci.* **10**, 3664–3684.
9. Roberts, W. M., Jacobs, R. A. & Hudspeth, A. J. (1991) *Ann. N.Y. Acad. Sci.* **635**, 221–233.
10. Gleisner, L., Flock, Å. & Wersäll, J. (1973) *Acta Otolaryngol.* **76**, 199–207.
11. Jørgensen, J. M. & Flock, Å. (1973) *J. Neurocytol.* **2**, 133–142.
12. Gulley, R. L. & Reese, T. S. (1977) *J. Comp. Neurol.* **171**, 517–544.
13. Hama, K. & Saito, K. (1977) *J. Neurocytol.* **6**, 361–373.
14. Hama, K. (1980) *J. Neurocytol.* **9**, 845–860.
15. Jacobs, R. A. & Hudspeth, A. J. (1990) *Cold Spring Harbor Symp. Quant. Biol.* **55**, 547–561.
16. Issa, N. P. & Hudspeth, A. J. (1994) *Biophys. J.* **66**, A379 (abstr.).
17. Minta, A., Kao, J. P. Y. & Tsien, R. Y. (1989) *J. Biol. Chem.* **264**, 8171–8178.
18. Roberts, W. M. (1993) *Nature (London)* **363**, 74–76.
19. Roberts, W. M. (1994) *J. Neurosci.* **14**, 3246–3262.
20. Balkema, G. W., Nguyen, H. T., Estrella, E. & Elwell, J. (1993) *Soc. Neurosci. Abstr.* **19**, 701.
21. De Virgilio, F., Steinberg, T. H. & Silverstein, S. C. (1990) *Cell Calcium* **11**, 57–62.
22. Michaelson, D. M., Ophir, I. & Angel, I. (1980) *J. Neurochem.* **35**, 116–124.
23. Srinivasan, Y., Elmer, L., Davis, J., Bennett, V. & Angelides, K. (1988) *Nature (London)* **333**, 177–180.
24. Kirsch, J., Wolters, I., Triller, A. & Betz, H. (1993) *Nature (London)* **366**, 745–748.
25. Miller, M. R. & Beck, J. (1988) *J. Comp. Neurol.* **271**, 604–628.
26. Sneary, M. G. (1988) *J. Comp. Neurol.* **276**, 588–606.
27. Storm, J. F. (1987) *J. Physiol. (London)* **385**, 733–759.
28. Augustine, G. J. (1990) *J. Physiol. (London)* **431**, 343–364.
29. Robitaille, R. & Charlton, M. P. (1992) *J. Neurosci.* **12**, 297–305.
30. Gola, M. & Crest, M. (1993) *Neuron* **10**, 689–699.
31. Robitaille, R., Garcia, M. L., Kaczorowski, G. J. & Charlton, M. P. (1993) *Neuron* **11**, 645–655.
32. Kros, C. J. & Crawford, A. C. (1990) *J. Physiol. (London)* **421**, 263–291.
33. Eatock, R. A., Saeki, M. & Hutzler, M. J. (1993) *J. Neurosci.* **13**, 1767–1783.